FLUID TRANSPORT IN A THICK LAYER ABOVE AN ACTIVE CILIATED SURFACE

NADAV LIRON, *Department of Applied Mathematics*
FRANK A. MEYER, *Department of Polymer Research, The Weizmann Institute of Science, Rehovot, Israel*

ABSTRACT The discrete cilia approach is employed to describe the flow field above an active ciliated surface in a layer of finite depth. The infinite-size cilia surface model predicts a uniform flow above the cilia surface. Modifications as a result of a finitely extending cilia surface inside a finite-size dish predict a backward parabolic profile above an active cilia surface. Experiments are described which demonstrate a good fit between theoretical predictions and observations. The results provide a sound physical basis for the proper interpretation of fluid-flow observations close to an active ciliary field.

INTRODUCTION

Much experimental and theoretical work on ciliary motion has been conducted in recent years. Several approaches have been proposed to depict ciliary motion and to model the resultant fluid motion of cilia-fluid interaction. The first model introduced was the "envelope model" in which the tips of the cilia are assumed to form a continuous waving envelope. The second model is the "cilia sublayer model" or "the discrete cilia model" in which each cilium is treated separately, and the contributions of all cilia are then summed up. The reader is referred to Blake and Sleigh (1) for a more detailed description of these models. The third approach models the cilia layer as a volume force distribution, see Keller et al. (2).

Most of these models were concerned with predicting propulsion of ciliated microorganisms, and only a few dealt with fluid propulsion by cilia. The discrete cilia model was introduced because of drawbacks with the envelope-model, and has been extensively discussed by Liron and Mochon (3) and Liron (4). In the first paper (3), propulsion velocity and fluid velocities were computed analytically and numerically, with cilia attached to an infinite plane in a regular array and the fluid extending to infinity above the plane. In the second paper (4), velocities were computed assuming the fluid is bounded above by another plane forming a channel. If the top plate is covered with cilia as well, this serves as a model for a ciliated tube. Fluid propulsion and velocity profiles can thus be computed. The velocity profile one gets inside the channel, in the pumping range, varies from a time-independent "backward" parabolic profile with possible backflow in the middle to a plug flow, depending on end-conditions.

In the discrete cilia model, each cilium is approximated by a distribution of force-singularities (Stokeslets) along its centerline and the contribution of all Stokeslets over all cilia

---

Dr. Liron's present address is Faculty of Mathematics, The Technion, IIT, Israel Institute of Technology, Haifa, Israel.

is summed up. The importance of the model is twofold: analytic expressions for the velocities, pressures, etc., can be obtained from which the qualitative behavior of the system is deduced; and velocities, pressures etc., can be predicted quantitatively once the kinematic description of the cilia is given. The ultimate success of a theoy is its ability to fit known experimental data, as well as to predict results of new experiments. In the present study, the discrete cilia model has been tested against experiments and found valid.

Experiments in closed ciliated tubes are difficult to perform and visualize. The approach usually used involves opening the tube and observing cilia beat and resultant fluid movement; see, for example, experiments quoted by Blandau (5).

In this study we have used tissue culture preparations of ciliated epithelium where the flow field can be conveniently visualized. The discrete cilia model was used to predict the flow field above a ciliated surface in a thick layer of fluid and the flow field due to a finite-size ciliated field bathed in a finite-size dish. The predictions of the model have been compared with experimental results. Two ciliated fields were used. One was an explant from the mucociliary epithelium of the frog's palate and the other was a monolayer cell outgrowth that develops from such explants. Different geometric configurations were required to view the ciliary-induced flow fields in the two cases, resulting in somewhat different experiments. The theoretical model for an infinite ciliated surface in a layer of fluid is first developed and the necessary important modifications due to the finite size of the ciliated surface and dish in which experimental observations were made are then introduced. A good fit between theory and experiment is demonstrated for both experimental setups.

EXPERIMENTAL

Biological Preparation

The mucociliary epithelium of the frog's palate, like that of mammalian mucociliary epithelia, consists of an outer layer of ciliated cells and goblet cells which secrete mucus, supported on a layer of loose connective tissue. The mucociliary epithelium of the frog's palate is used in feeding; food particles trapped on the mucus layer are transported by ciliary action into the gullet. The mucociliary membrane (epithelium and supporting connective tissue) of the frog palate can be easily excised and prepared as explants or as cell monolayer outgrowths suitable for microscopic visualization of ciliary-induced flow fields. In these preparations mucus "droplets" secreted from the goblet cells into the medium are seen, but no mucus layer covering the cilia forms. The ciliary-induced flow field set up in the bathing medium, therefore, can be studied unhindered.

The preparations were obtained essentially following the procedure of Nevo et al. (6) under sterile conditions. The mucociliary membrane of the frog's (*Rana esculenta*) upper palate was excised and transferred to amphibian phosphate-buffered saline (NaCl – 0.15 M, 720 ml; KCl – 0.150 M, 32 ml; phosphate buffer (Na_2HPO_4/KH_2PO_4) –0.067 M, 48 ml, pH 7.5; distilled water 200 ml) containing the antibiotics penicillin (1,000 IU/ml), kanamycin (500 μg/ml), and mycostatin (100 IU/ml) to prevent bacterial growth. As much as possible of the blood vessels and loose connective tissue was gently scraped off from the inner side. Small pieces (1–2 mm^2) were excised along a path of the tissue where cilia beat in the same direction (the central depression running from the outer periphery to the gullet [7]). Tissue pieces were washed with four changes of the above solution. Each explant was placed with mucociliary epithelium uppermost on an oblong glass support (3.4 × 0.55 cm) close to one of the long edges and orientated such that ciliary beat direction was parallel to it. Tissue pieces on their supports were placed in separate plastic culture dishes (Nunc Products, DK-4000 Roskilde, Denmark) and culture medium (65% Leibowitz medium L-15 [Grand Island Biological Company, Grand Island, New Yórk], 15% fetal calf serum and 20% distilled water; containing 100 IU penicillin/ml and 100 μg/ml each of kanamycin

and mycostatin; pH 7.4) was added to a depth just enough to cover the tissue. Cultures were kept at room temperature (between 21° and 24°C) in air. After 2 d, explants had attached to their supports and could then be mounted for flow-field visualization studies.

Explants cultivated for monolayer outgrowths were prepared as above from tissue pieces placed in the center of small coverslips. After attachment, a further period of 6 d was required for suitable monolayer outgrowths to be formed. During this time the medium was replaced every other day by sufficient fresh medium to nearly fill the culture dish. The development of monolayer outgrowths was monitored *enface* with transmitted light in a Nikon phase-contrast inverted microscope (Nippon Kogaku K.K., Tokyo, ×400). Outgrowths which had formed a sheet of flattened cells extending several millimeters from the explant and around it were used. In such preparations, a degree of coordination of the metachronic wave of adjacent ciliated cells forming a continuous wave had developed in several patches within the monolayer.

Flow Measurements

Explants were not sufficiently transparent for the mucociliary region to be viewed *enface* with transmitted light. Therefore, the support carrying the attached explant was mounted on the edge where the tissue had been placed, in the culture dish as shown in Fig. 1 *a*. The support with explant was secured using two clips resting on the lip of the dish. Where necessary, culture medium was added to cover the explant. In this configuration, the mucociliary epithelium can be viewed side-on with transmitted light in the phase-contrast microscope. The placement of the explant on the support initially ensured that the tissue would be within the working distance of the microscope with the ciliary-induced flow field parallel to the floor of the culture dish. The monolayer outgrowths were sufficiently transparent for the induced flow field to be readily visualized *enface* (Fig. 1 *b*).

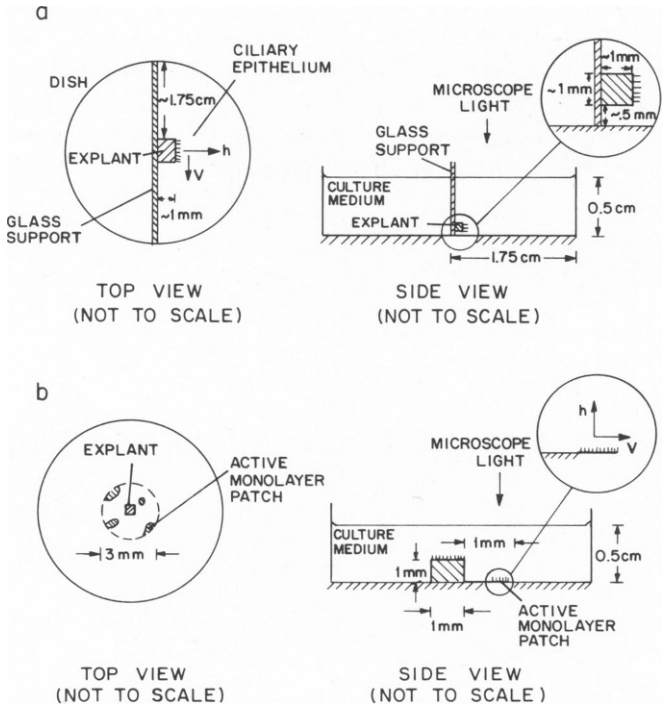

FIGURE 1 Experimental set up of the ciliary layer in the culture dish. (*a*) explant, (*b*) monolayer outgrowth. Figures not to scale. Observations are performed using a phase-contrast inverted microscope (×400).

The ciliary-induced flow in the medium at various distances normal to the ciliary field was determined under the microscope by timing the passage of 1-μm diameter polystyrene latex particles (Dow Corning Corp., Midland, Mich.) along a 30-μm path line parallel to the plane of the beating cilia (Fig. 1 *a, b*). For each distance normal to the ciliary plane, six measurements of velocity were performed and their mean with standard deviation calculated. Distances were determined with the aid of an eyepiece micrometer disk inscribed with a grid that had been calibrated against a stage micrometer. Distances normal to the monolayer were determined by the vertical advancement of the microscope stage from the plane of the ciliary tips to the particular height being focused on.

Ciliary-induced flow over the monolayer outgrowths was less uniform in direction than that for the explant because different ciliated patches in the monolayer beat in somewhat different directions. Therefore, measurements were only performed over patches that were relatively isolated and that were particularly active. For these patches the direction of the flow field remained unaltered with distance above the beating ciliary tips.

THEORY

Two configurations have been used in the experiments. In one case using explants, there is an array of cilia with a far away wall, the culture dish wall, in the direction normal to the ciliary layer. In the other case, using monolayer ciliated patches, there is a far away free surface in the direction normal to the ciliary layer. Because previous modeling has not dealt with free-surface problems, we shall expand first on this aspect.

Infinite-Size Model

We consider a regular array of cilia with bases regularly spaced in a two dimensional rectangular lattice with spacings (a,b) on an infinite plane defined by $x_3 = 0$, (x_1, x_2, x_3) Cartesian coordinates (Fig. 2). It is assumed that the cilia beat (essentially) in the direction of increasing x_1, and that a metachronal wave is propagating in the (positive or negative) x_1-direction, such that the wavelength is $m_0 a$. The problem is to solve for the flow field, which can be taken as Stokes flow with the boundary conditions

$$\mathbf{u}\ (\text{cilium}) = \text{observed velocity}, \tag{1}$$

and on $x_3 = \xi(x_1, x_2)$, the free surface,

$$\sigma_{x_1,x_3} = \sigma_{x_2,x_3} = \sigma_{x_3,x_3} = 0, \tag{2}$$

$$u_3(\xi) = u_1 \frac{\partial \xi}{\partial x_1} + u_2 \frac{\partial \xi}{\partial x_2}, \tag{3}$$

where σ_{x_3,x_3}, σ_{x_1,x_3}, σ_{x_2,x_3} are the normal and shear stresses, respectively, and $\mathbf{u}$ the velocity vector.

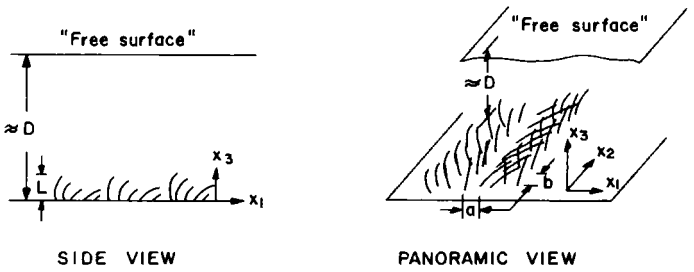

FIGURE 2 The model of cilia distribution, side and panoramic views.

We assume that the free surface is at $x_3 = D$ when the cilia are immobile, and that $D \gg L$, L the cilium length, i.e., we have a thick-layer fluid.

In the discrete cilia model one replaces each cilium by a Stokeslet distribution along its centerline and then sums overall cilia, see Blake (8), Liron and Mochon (3), and Liron (4). Two difficulties emerge when one tries to implement this idea here. The first is that unlike the cases of flow between rigid boundaries (or infinity), the shape of the free surface is part of the problem and will be different for a different distribution of Stokeslets. The second difficulty derives from the first in that one could superpose if one knew the final free-surface shape which unfortunately one does not. Strictly speaking, one cannot therefore use the principle of superposition. For a thick layer of fluid, though, we have a very good approximation for the free surface which is

$$\xi \equiv D. \tag{4}$$

Firstly, as has been shown in previous cases, the model yields a periodic flow with a period of the metachronal wavelength $m_0 a$ which is usually of the order of 20 μm. Thus, the free surface will also be periodic with the same period, and because this period is assumed very small compared with thickness of the layer, we expect perturbations from $\xi = D$ to be small. Moreover, the approximation (4) implies that

$$u_3 = \frac{\partial u_1}{\partial x_3} = \frac{\partial u_2}{\partial x_3} = -P + 2\mu \frac{\partial u_3}{\partial x_3} = 0, \tag{5}$$

on $x_3 = D$ for $\xi = D$ to be "exactly" the free surface. Here P is the pressure. If P and $\mathbf{u}$ are exponentially small at $\xi = D$ then indeed we expect this to be a good approximation of the free surface.

To see that this is indeed the case we have to consider an infinite array of Stokeslets all of the same strength and pointing in the same direction, with spacing $m_0 a$ in the x_1-direction, spacing b in the x_2-direction, and height $x_3 = h$ above the surface, (see the kernels in Liron and Mochon [3] and Liron [4]).

Two approximations are plausible. The first uses the Stokeslet solution in infinite medium above a flat plate. In this case all velocities and pressure, and their derivatives decay exponentially, as $\exp[-(x_3 - h)\, 2\pi/m_0 a]$ except for the velocity parallel to the plate, u_1, which approaches a constant value exponentially. For an example of expressions one gets, see Appendix. The second possible approximation is to use Stokeslets between two parallel flat plates a distance $2D$ apart, adding to each Stokeslet its image by reflection in the plane $x_3 = D$ (Fig. 3). This is somewhat better than the previous approximation in that we have $u_3 \equiv 0$, as well as

$$\frac{\partial u_1}{\partial x_3} = \frac{\partial u_2}{\partial x_3} = \frac{\partial u_3}{\partial x_3} = 0; \text{ on } x_3 = D, \tag{6}$$

and we must choose the kernel in Liron (4) such that the pressure rise per wavelength is zero. It then follows that the pressure is exponentially small on $x_3 = D$, being of the order of $\exp[-(D-h)\, 2\pi/m_0 a]$ as in the first approximation. For the solution due to a Stokeslet between parallel plates, see Liron and Mochon (9).

It follows that if we have a cilia surface extending to infinity in a deep layer, the only

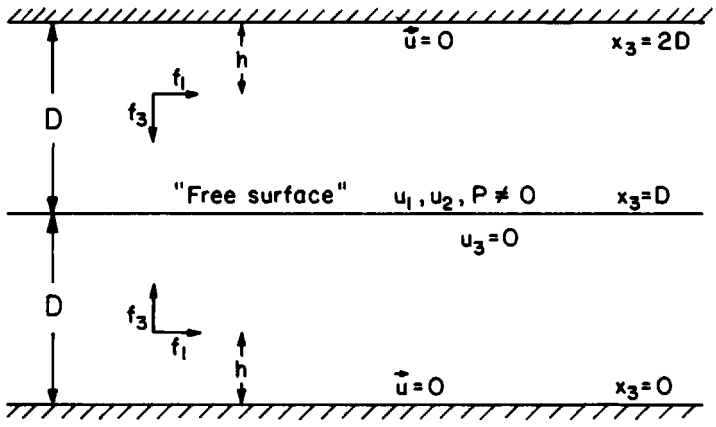

FIGURE 3 Stokeslet with reflection in the midplane approximating the free surface.

possible solution is a local flow above the cilia layer, in the direction of beat, decaying exponentially away from it, or more generally a flow in the direction of beat blending exponentially into a uniform (plug) flow above it. It should be emphasized that the theory predicts time-dependent velocity up to a height of a few cilia lengths and a practically time-independent flow further up. In the experiments, though, we do not have an infinite layer, but a finite-size tissue placed in a finite-size dish. The effects of these changes are discussed below.

Finite Tissue (or Layer) in a Dish

Typically, experiments were done on ciliated preparations of ~ 0.1-cm in diameter in a 3.5-cm diameter dish, with a 0.5-cm fluid depth. Thus, the tissue is of finite size and is in a finite-size dish (see Fig. 1) and the infinite-size model must obviously be modified. The flux of fluid in the direction of beat is positive in the infinite model, whereas it is clear that the flux inside the dish through the entire width is zero.

A finite-size tissue placed on a plane extending to infinity will act as a concentrated force if looked at from far away. As the flux is zero, one would expect to see a circulation similar to the circulation caused by a Stokeslet parallel to and in-between two plates (Fig. 4). Locally, however, if the dimension of the tissue is W and we look at a height x_3 above the tissue such that $L \ll x_3 \ll W$, where L is the cilium length, we expect to see a uniform flow as predicted from the infinite tissue case together with modifications due to the finite dish. The flow of fluid along the tissue is partly compensated by backflow along the sides of the tissue, altogether causing a circulation of fluid. Together with the flow of fluid along the tissue there will be a pressure difference between the "forward end" (in direction of beat) and the "back end," (just as for a concentrated force) which is height-independent. In the infinite dish case, with the cilia layer parallel to the bottom, one can see this pressure difference as driving the fluid back along the sides. In the finite-dish case there is not enough lateral distance for the fluid to move back along the sides of the tissue (likewise in the case of cilia patch normal to the bottom), and part will move back along the tissue. Thus, the fluid moving back above the tissue is driven by a pressure difference which in the range of $L \ll x_3 \ll W$ is independent of x_3 in the central region of the tissue and we expect a "backward" parabolic profile with x_3 in this

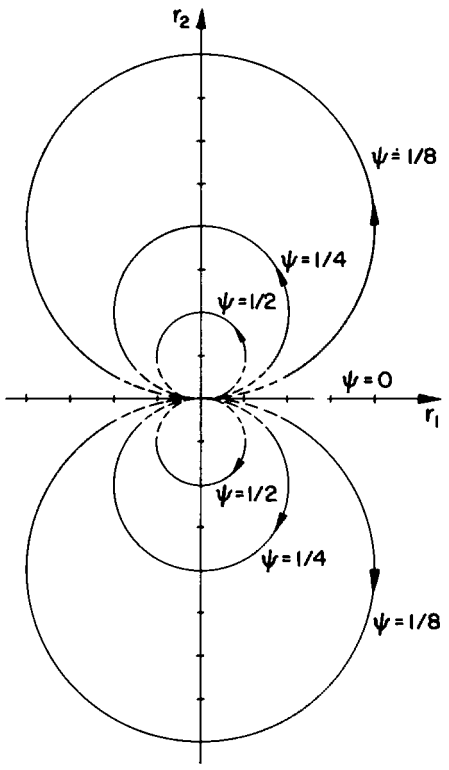

FIGURE 4 Far field streamlines ψ = constant, for a Stokeslet between two parallel plates a distance H apart situated at $r_1 = r_2 = 0$, and height ξ/H, pointing in the r_1-direction. ψ in units of $(3/2\pi\mu H)\xi/H(1 - \xi/H)x_3/H(1 - x_3/H)$, x_3 the height above the bottom plate.

region for the longitudinal velocity, i.e., a local Poiseuille-type flow together with a shear flow. The strength of this parabolic profile will be more prominent the smaller the size of the dish relative to the tissue size in the monolayer experiments, and the shallower the depth of the fluid in the cultivated explant experiments. In other words, the strength of the parabolic profile, one would expect, will depend on the extent of lateral distance on the sides of the cilia patch, available for recirculation. One should emphasize that this time-independent parabolic profile is to be expected in the range $L \ll x_3 \ll W$, and where disturbances due to other patches of active cilia are negligible.

RESULTS

According to the theoretical discussion above, we expect to see a time-independent parabolic profile for the velocity above the cilia, with higher velocity closer to the cilia, and lower velocity further away, i.e., a backward parabolic profile, if forward is the direction of cilia beat. This, in the region $L \ll x_3 \ll W$. Also, as already discussed, the strength of the parabolic profile depends, among other things, on the lateral distance available, as well as the distance to the walls. We thus chose to measure velocities in the range $L \ll x_3 \ll W$, and fit a parabola to the experimental results, using a least-squares procedure.

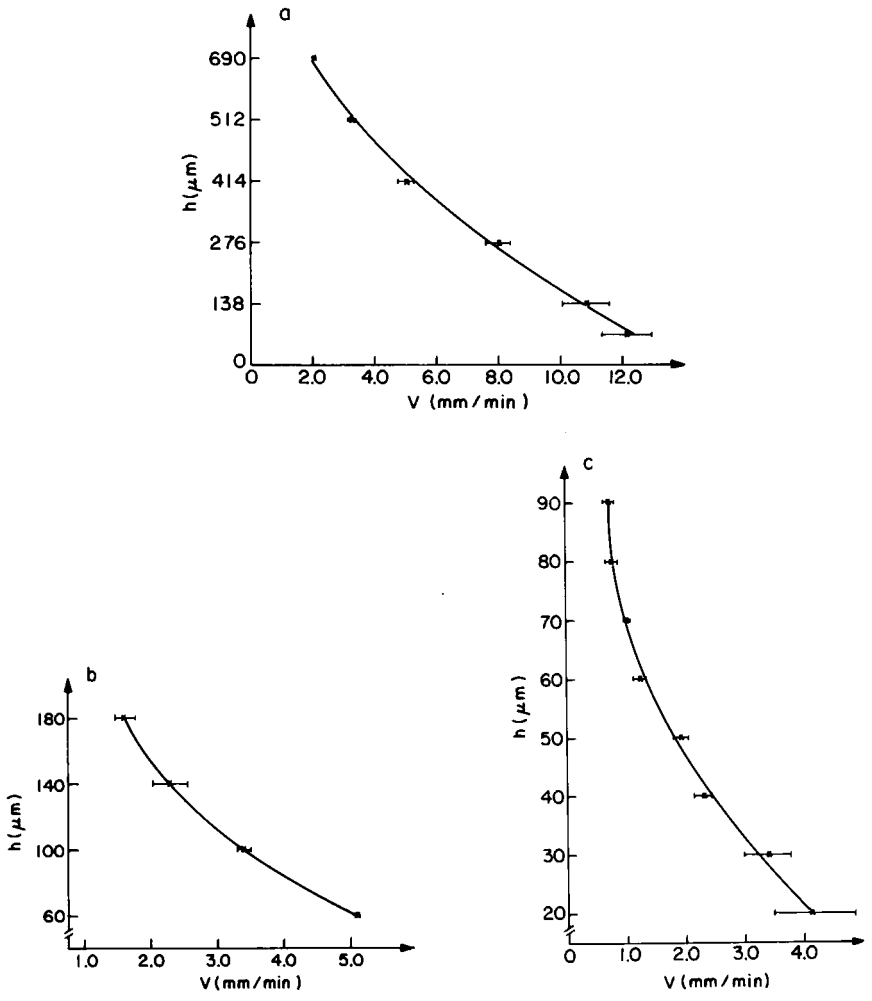

FIGURE 5 Velocity profiles V in millimeters per minute with height h in micrometers above the cilia tips for (*a*) flow above a tissue explant, (*b, c*) flow above monolayer outgrowths. Error bars on experimental results indicate standard deviation and the smooth curve is a least-squares parabolic fit.

Three sets of experiments are shown in Fig. 5 *a–c*. Fig. 5 *a* shows the results of fitting a parabola through six points, for the experiment with the explant (Fig. 1 *a*). As the tissue is ~1 mm in length and 1–2 mm^2 in area, the range $x_3 \ll W$ for which we expect to see a parabolic profile is of the order of several hundred micrometers. Indeed, a good fit is obtained over the entire range of heights, from 69 to 690 μm above the ciliary layer. Fig. 5 *b, c,* shows the fit for experiments using two different monolayer outgrowths with four and eight experimental points respectively. Because coordination of cilia in the monolayer outgrowths is restricted to much smaller areas than in the explant, the fit is accordingly to smaller heights above the cilia; 180 μm in Fig. 5 *b* and 90 μm in Fig. 5 *c*. Although three points determine a parabola, it is still striking that the fourth point in Fig. 5 *b* falls directly on the line determined by the other three. A very nice fit is also seen in Fig. 5 *c,* where measurements are made at smaller

intervals (10 μm). It should be noted that the axis of the parabola lies far below the value of 5,000 μm in Fig. 5 *b, c*, which is the free-surface height, and would be expected to be the axis position in the infinite layer case.

DISCUSSION

The discrete cilia approach has been used earlier (3, 4) to predict propulsion velocity of ciliated microorganisms, as well as to obtain velocity profiles due to cilia beat in a channel. As there is no formal mathematical proof that replacing each cilium by a Stokeslet distribution along its centerline is adequate, it is important to check whether such a model yields the correct behavior of the flow fields and in particular the global aspects of the flow. It is also well known that Stokeslets alone are not sufficient to accurately represent the cilium-fluid interaction close to the cilium.

In the present study, we have presented a combined theoretical and experimental study of the flow field above a ciliated surface, where we have used the discrete cilia approach. The free surface complicates the problem as direct superposition is not, strictly speaking, correct. If the layer of fluid is deep enough, relative to the cilia lengths, then approximating the free surface by a plane of constant height is seen to be a good approximation. The superposition, or interference, of Stokeslets solutions for an array of Stokeslets in semi-infinite medium, or in-between two plates, decays exponentially with height above the cilia surface, and is a good approximation to the "correct" Stokeslets solution.

As the infinite-size model predicts an exponential decay of all velocities due to Stokeslets, except for u_1 which approaches a constant (possibly nonzero), we would expect to see a uniform flow if we look several cilium lengths above the cilia surface. However, the finite-size of the tissue, as well as of the dish in which it is placed play an important role as well. Consider the case where the cilia surface fills the entire bottom of the dish. As the flux is obviously zero in the direction of beat, and we are forcing fluid forward near the cilia surface, the fluid will flow back higher up, and we get a backward parabolic profile far from the walls. If the cilia surface is smaller than the dish size, part of the backflow will take place on the sides of the cilia surface, as well as above it, and the smaller the size of the surface, the more the flow on the sides. The Stokeslets induce a pressure difference between the front of the cilia layer and the back (in the direction of cilia beat). This pressure difference can be looked upon as the driving force for the return flow.

The predicted time-independent backward parabolic profile is expected only in the range $L \ll x_3 \ll W$, where L is the cilium length and W is the diameter of the cilia layer. Thus, the axis of the parabola which is expected to lie on the free surface in the infinite layer model does not do so in the experimental results. Although the present modeling is not detailed enough to allow for quantitative comparisons, it does provide a sound physical basis for proper interpretation of microscopic observations close to cilia patches, or layers. In particular, the theoretical discussion indicates that the observed parabolic profile is not due to any particular type of cilia beat, but rather an interaction between the ciliary layer and the finite dish, the latter forcing a zero flux condition, and consequently a pressure head between front and back of the cilia layer, creating a flow in the opposite direction.

The experimental results derive in part from work supported by grant NS 10048 from the National Institutes of Health.

Received for publication 15 June 1979 and in revised form 20 November 1979.

APPENDIX

For an infinite array of regularly spaced Stokeslets above an infinite plate, velocities and pressure decay exponentially with height above the plate. If the Stokeslets coordinates are $(\xi_1 + n(m_0a), \xi_2 + mb, h)$ $n = 0, \pm 1, \pm 2, \ldots$ $m = 0, \pm 1, \pm 2, \ldots$ with the plate at $x_3 = 0$, and we have $\xi_1 + n_1(m_0a) \le x_1 < \xi_1 + (n_1 + 1)m_0a$, $\xi_2 + m_1b \le x_2 < \xi_2 + (m_1 + 1)b$, then as an example, the pressure due to the above Stokeslets array, each of unit strength, pointing in the x_1-direction is

$$P_1(x_1, x_2, x_3) = \frac{8\pi}{(m_0a)^2} \sum_{n=-\infty}^{\infty} \sum_{\ell=1}^{\infty} \ell \sin(2\pi\ell r_1/m_0a)\left[K_0\left(\frac{2\pi\ell\rho_1}{m_0a}\right) - K_0\left(\frac{2\pi\ell\rho_2}{m_0a}\right)\right] \quad \text{(A1)}$$

$$+ \frac{32\pi^2h(x_3 + h)}{(m_0a)^3} \sum_{n=-\infty}^{\infty} \sum_{\ell=1}^{\infty} \ell^2 \sin(2\pi\ell r_1/m_0a)\, K_1\left(\frac{2\pi\ell\rho_2}{m_0a}\right)\Big/\rho_2.$$

Here

$$r_1 = x_1 - \xi_1 - n_1m_0a, \qquad r_2 = x_2 - \xi_2 - m_1b. \quad \text{(A2)}$$

Also

$$\rho_1^2 = \rho_1^2(n) = (r_2 + nb)^2 + (x_3 - h)^2, \quad \text{(A3)}$$

$$\rho_2^2 = \rho_2^2(n) = (r_2 + nb)^2 + (x_3 + h)^2.$$

K_0 and K_1 are Bessel functions, which decay exponentially with their argument. Thus,

$$P \sim \exp[-(x_3 - h)\, 2\pi/m_0a], \qquad x_3 \gg h. \quad \text{(A4)}$$

REFERENCES

1. BLAKE, J. R., and M. A. SLEIGH. 1974. Mechanics of ciliary locomotion. *Biol. Rev. Camb. Philos. Soc.* **49**:85–125.
2. KELLER, S. R., Y. T. WU, and C. BRENNEN. 1975. A traction-layer model for ciliary propulsion. *In* Proceeding of the Symposium on Swimming and Flying in Nature. T. Y. Wu, C. J. Brokaw, and C. Brennen, editors. Plenum Publishing Corporation, New York. 253–271.
3. LIRON, N., and S. MOCHON. 1976. The discrete-cilia approach to propulsion of ciliated micro-organisms. *J. Fluid Mech.* **75**:593–607.
4. LIRON, N. 1978. Fluid transport by cilia between parallel plates. *J. Fluid Mech.* **86**:705–726.
5. BLANDAU, R. J. 1969. Gamete transport—comparative aspects. *In* The Mammalian Oviduct. E.S.E. Hafez and R. J. Blandau, editors. University of Chicago Press, Chicago. 129–162.
6. NEVO, A. C., Z. WEISMAN, and J. SADÉ. 1975. Cell proliferation and cell differentiation in tissue cultures of adult mucociliary epithelia. *Differentiation.* **3**:79–90.
7. SADÉ, J., N. ELIEZER, A. SILBERBERG, and A. C. NEVO. 1970. The role of mucus in transport by cilia. *Am. Rev. Respir. Dis.* **102**:48–52.
8. BLAKE, J. R. 1972. A model for the micro-structure in ciliated organisms. *J. Fluid Mech.* **55**:1–23.
9. LIRON, N., and S. MOCHON. 1976. Stokes flow for a Stokeslet between two parallel flat plates. *J. Eng. Math.* **10**:287–303.